

A Shock Tube Study of the Vibrational and Chemical Relaxation of Nitric Oxide at High Temperatures*

Kurt L. Wray and J. Derek Teare

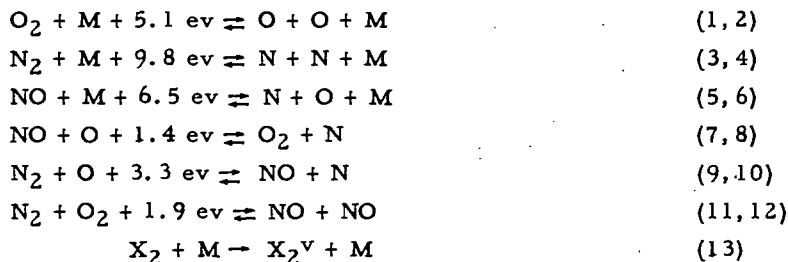
Avco-Everett Research Laboratory
Everett 49, Massachusetts

Introduction

Extensive studies of the relaxation region behind normal shocks in air have been carried out at this Laboratory.⁽¹⁾ The experiments include studies on pure air, N₂, O₂, NO, and various mixtures of these with each other and with argon. As a part of this program, we have undertaken a study of the chemical kinetics of NO in the temperature range 3000 - 8000° K, and of the vibrational relaxation of NO in the range 1500 - 7000° K. The experimental technique employed in this investigation was the monitoring of the NO concentration as a function of time by its absorption of 1270 Å radiation. The present paper will be restricted to this portion of the overall program, and to a discussion of those reactions which involve the formation, removal or vibrational relaxation of NO.

As we shall see, such systems at high temperatures are fairly involved, and the analysis of the experimental data requires the aid of an electronic computer. To this end, computer programs using an IBM 704 have been written which permit the calculation of the density, temperature, and concentration time history for any given set of pertinent rate constants. These programs include a postulated coupling of vibrational and dissociative processes.⁽²⁾

The following is a list of chemical reactions occurring in air which are pertinent to this paper:



It should be pointed out that the collision partner "M" can be any molecule or atom, and part of the unravelling of the kinetics is to evaluate the relative efficiencies of the possible catalysts. Reaction 1, 2 has been studied extensively by Camac and Vaughan⁽³⁾ and others, and the rate constants are well determined. Reaction 3, 4 plays but a minor role even at the highest temperatures encountered

*Supported jointly by AFBMD-ARDC-USAF, Contract AF 04(647)-278 and ARPA, monitored by the ARGMA-AOMC-U. S. Army, Contract DA-19-020-ORD-4862.

in the experiments under discussion. Reactions 5-12 all contribute to the formation and subsequent removal of NO behind a shock front in air. Rate constant information for these reactions has been obtained from observations of the decomposition of shock-heated NO.

Vibrational relaxation (reaction 13) plays an important role early in the time history following the shock front. The vibrational relaxation of O₂ and N₂ has been measured by other workers.^(4, 5) Robben⁽⁶⁾ has measured the vibrational relaxation rate of NO by NO over the temperature range 400 - 1500° K.

Theory of Vibrational Relaxation

It was assumed by Bethe and Teller,⁽⁷⁾ and subsequently proven by Montroll and Shuler⁽⁸⁾, that if a gas initially has a Boltzmann distribution of vibrational energies, it will relax to a final Boltzmann distribution of energies with all intermediate stages having a well defined vibrational temperature.

The relaxation equation given by the above authors is remarkably simple when written in terms of vibrational energy. If the gas is initially at room temperature, we can write

$$\frac{d \log_e (1 - E_v/E_f)}{dt} = -\frac{1}{\tau} \quad (14)$$

and, for an harmonic oscillator, we obtain from statistical mechanics

$$\frac{E_v}{E_f} = \frac{e^{\Theta/T_f} - 1}{e^{\Theta/T_v} - 1} \quad (15)$$

In these equations, E_v is the vibrational energy corresponding to the vibrational temperature T_v at time t , E_f is the vibrational energy corresponding to the final vibrational temperature T_f and τ is the relaxation time. For NO, $\Theta = 2688^\circ$ K.

The relaxation time, τ , is related to a transition probability by the equation

$$\frac{1}{\tau} = Z P_{10} (1 - e^{-\Theta/T}) \quad (16)$$

where T is the translational temperature, P_{10} is the transition probability per oscillator per collision for transition between vibrational levels 1 and 0, and Z is the number of collisions suffered by a single oscillator molecule per second with a catalyst particle.

For an NO-Ar mixture, in which two catalytic species are present, the effective relaxation time is related to the relaxation time for each individual catalyst by the equation

$$\frac{1}{\tau} = \frac{f}{\tau_{\text{NO-NO}}} + \frac{1-f}{\tau_{\text{NO-Ar}}} \quad (17)$$

in which f is the fraction of oscillator molecules in the mixture.

Theoretical formulae for P_{10} have been proposed by Landau and Teller⁽⁹⁾ and by Schwartz, Slawsky and Herzfeld.⁽¹⁰⁾ The SSH theory allows P_{10} to be calculated using the Lennard-Jones parameters ϵ and r_0 .

$$P_{10} = A e^{-BT^{-1/3}} \quad (18)$$

where, for most molecules A and B are weak functions of temperature.

Experimental Program

The ultraviolet light absorption technique employed in these studies is similar to that used by Davidson and his co-workers⁽¹¹⁾ who used visible light to measure iodine relaxation rates. Camac⁽⁵⁾ has developed the technique extensively using radiation at 1470 Å in his O₂ studies. Watanabe, et al,⁽¹²⁾ have measured the room temperature absorption coefficients for several gases in the vacuum ultraviolet and found a narrow window in the absorption spectra of O₂ at 1270 Å where NO showed strong absorption. Since, in this investigation, we wanted primarily to observe the NO molecule, we chose to work at a wavelength of 1270 Å with a bandwidth of 5Å.

A schematic diagram of the apparatus is shown in Fig. 1. The shock tube, constructed of stainless steel, was of a circular cross-section having an inside diameter of 3.81 cm. Scored stainless steel diaphragms were used, and they were ruptured by increasing the driver pressure until the diaphragm failed. The usual driver gas was hydrogen or a mixture of hydrogen and nitrogen. The shock speed was determined by means of platinum strip heat transfer gages. The measurements of the position of the shock front could be made to about 1/3 microsecond, which corresponded to 0.3% uncertainty in the shock velocity.

The optical observation station at the shock tube consisted of the following components: (1) light source, (2) slits and CaF₂ windows on both sides of the shock tube, (3) monochromator, (4) phosphor-coated photomultiplier, and (5) recording oscilloscope.

Two types of light sources were used. When it was desired to observe the shock-heated gas for relatively long times, a hydrogen discharge lamp was employed. This lamp produced several strong molecular lines in the 5Å wavelength band centered on 1270 Å; its intensity which decayed monotonically to zero in about 3 milliseconds allowed a resolution of about 1 μ sec.

When it was desired to observe the leading edge of the shock front, a Lyman lamp was used. The Lyman lamp is a helium discharge light source and it produces a continuum in the wavelength region of interest. This lamp produced a damped oscillating output whose second cycle (the one used) allowed a testing time of about 15 μ sec and was sufficiently intense to allow resolution of a few tenths of a microsecond.

An oscillogram obtained with the U. V. absorption apparatus is shown in Fig. 2. This oscillogram is reproduced here to show the time history over the entire testing time; it does not have a sufficiently fast sweep speed to show the relaxation phenomenon to maximum advantage.

The ground state absorption coefficients for NO, O₂ and N₂ (i.e., room temperature absorption) were determined in this apparatus using the hydrogen lamp on a DC basis with the output of the photomultiplier being monitored by a microammeter, the NO and O₂ gases being introduced into the shock tube. In the case of N₂, however, the absorption by the room temperature gas was insufficient and the path length was increased by introducing the gas into the monochromator.

It was necessary to experimentally determine the absorption coefficients for the various species as a function of vibrational temperature. For this purpose, many shock tube runs were made with NO-Ar and O₂-Ar mixtures and pure N₂. The absorption by the shock-heated gas was measured at a point on the oscillogram corresponding to complete vibrational relaxation but before dissociation starts.

The temperature (vibrational) and density corresponding to this condition were calculated for each run and were used in conjunction with the oscillograms to obtain the curves shown in Fig. 3. The two points at the extreme left of these curves are the room temperature absorption coefficients. We see that vibrationally excited NO absorbs more strongly than does the ground state and that the absorption seems to increase roughly linearly with increasing vibrational temperature. Notice that the absorption coefficient for vibrationally excited O_2 is much larger than for the ground state. This is somewhat unfortunate because it means that under certain conditions (early times in air) the correction for the absorption due to the vibrationally excited O_2 becomes significant.

Although the absorption coefficient of N_2 is completely negligible at room temperature ($k = .014 \text{ cm}^{-1}$), our experiments showed it to be a strong function of vibrational temperature ($k = 1.1$ at 6000°K , 3.6 at 8000°K). This absorption correlates with the population of the 11th vibrational state. Vibrationally excited nitrogen thus contributes significantly to the absorption in shock heated air above 6000°K .

By observing the magnitude of the initial jump in the signal due to the compression across the shock front, it was proven that the absorption coefficient is independent of translational and rotational temperature.

Data Reduction

For the purpose of the chemical relaxation studies, computed curves were fitted to a total of 42 experimental time histories in the following six mixtures: 1/2% NO, 1/2% NO + 1/4% O_2 , 50% NO, 10% NO, 100% air and 20% air, in all cases the diluent being argon. The temperature range covered was $3000 - 8000^\circ \text{K}$.

The general equation for the intensity of monochromatic radiation, I , transmitted through a gas sample is

$$I/I_0 = \exp \left\{ - L (P_1/P_s) \cdot x(\rho_2/\rho_1) \sum_j (k_j f_j) \right\} \quad (18)$$

where I_0 is the intensity of radiation with no absorber in the optical path of length L , P_1 is the total initial pressure of the gas, P_s is standard pressure, ρ_2/ρ_1 is the density ratio across the shock, and k_j is the absorption coefficient of species j having a concentration f_j (moles/original mole of mixture).

In general, the density ratio and the quantities k_j and f_j vary throughout the relaxation period. Their values are obtained from a computer program which integrates the chemical and vibrational rate equations subject to the constraints imposed by the conservation equations. The computer output includes T , ρ_2/ρ_1 , f_j and df_j/dt , as well as I/I_0 which is used for direct comparison with experimental intensity vs. time histories. The input to the computer includes shock speed, composition, initial pressure, k_j as a function of T_v for the three absorbing species, together with the rate constant information for reactions 1-13. The rate constants for equations 5-12 were varied in a systematic trial and error process which yielded a set of rate constants which satisfactorily fit all the measurements. The high temperature vibrational relaxation rates for NO required in the above computer program were obtained independently as discussed below.

Three NO-Ar mixtures (50% NO, 10% NO and 1% NO) were analyzed for vibrational rate information. The experimental signal (I/I_0) must be related to the quantity $1 - E_v/E_f$, using the NO absorption coefficient of Fig. 3. For each run analyzed it was necessary to construct a plot of I/I_0 vs. $(1 - E_v/E_f)$, and then to cross-plot the I/I_0 vs. time data from the oscillogram. Two typical oscillograms obtained for vibrational analysis are shown in Fig. 4, and the corresponding cross-plots are given in Fig. 5.

According to Eq. 14 such a plot should be a straight line. In general, all the data yielded fairly straight lines when plotted in the above manner. Although these lines seldom went through the value of unity at $t = 0$, the discrepancies were consistent with transit time considerations. The slopes of these straight lines give the vibrational relaxation (laboratory) time.

Following the usual practice, the data will be presented with the relaxation times in the particle coordinate system and normalized to standard density. In Fig. 6 we have plotted $\tau_s (1 - e^{-\Theta/T})$ vs. $T^{-1/3}$ for the three mixtures studied.

Results and Conclusions

The results of our vibrational relaxation experiments as well as those of Robben⁽⁶⁾ indicate that the Lennard-Jones parameters appropriate to an NO collision leading to vibrational relaxation are $r_0 = 2.15$ Å and $\epsilon/k = 2000^\circ$ K. For this exceptionally high value of ϵ the usual statement that a plot of $\log \tau_s (1 - e^{-\Theta/T})$ vs. $T^{-1/3}$ should yield a straight line is not valid.

The three solid lines in Fig. 6 are least square fits to the data based on Eq. 17. The curvature in these lines is produced by temperature dependent terms in P_{10} that for most molecules are insignificant compared to the $T^{-1/3}$ dependence. The two dashed curves in Fig. 6 labelled $f = 1$ and $f = 0$ are the computed relaxation times for the NO-NO and the NO-Ar collision, respectively, based on the least square fit to the experimental data.

The above relaxation times can be converted into transition probabilities by means of Eq. 16. The calculated probabilities resulting from these experiments are plotted vs. $T^{-1/3}$ in Fig. 7. They are the solid lines labelled $P_{\text{NO-NO}}$ and $P_{\text{NO-Ar}}$. It should be pointed out that the $P_{\text{NO-NO}}$ curve is very nearly the curve one would get using the data from the NO-rich mixtures alone and assuming that the argon plays no role in exciting the NO. The $P_{\text{NO-Ar}}$ curve, on the other hand, is obtained essentially from the 1% data only after subtracting out the large effect due to NO-NO collisions. Hence, the uncertainty in this curve is much greater than the $P_{\text{NO-NO}}$ curve. For comparison, Robben's data is also shown in Fig. 7. It covers the temperature range from 400 - 1500° K.

The other two curves shown in this figure are calculated from the SSH theory⁽¹⁰⁾ for the Lennard-Jones parameters indicated in the figure. The lower of these two curves should apply to both NO-NO and NO-Ar transition probabilities.

Robben pointed out in his paper that there is evidence of the formation of an NO dimer (of rectangular geometry) in the solid and liquid state.^(13,14) The Lennard Jones parameters appropriate to the dimer were the ones used to calculate the upper theoretical curve. The low temperature portion of this curve has been drawn as a dotted line as some of the approximations in the SSH theory are not applicable in this temperature range for $\epsilon/k = 2000^\circ$ K.

At high temperatures the slope of the theoretical curve based on the dimer potential compares well with the experimental one. Since the dimer has rectangular geometry, an attractive collision could result only for specifically oriented collision pairs, and a steric factor of about 1/30 implied by Fig. 7 is not unreasonable.

The noise fluctuations in the oscilloscope traces, which were of statistical origin, could produce errors in I/I_0 of as much as $\pm 4\%$. This probably represents the greatest source of scatter in the vibrational data, introducing somewhat less than a factor of 2 uncertainty in the relaxation times.

The various mixtures used in the chemical relaxation studies were chosen to emphasize the relative contribution of particular reactions. For example, the

1/2% NO runs provided a determination of the argon contribution to reaction 5, while the 1/2% NO + 1/4% O₂ mixture was used (at Prof. Norman Davidson's suggestion) to emphasize the importance of reaction 7 by providing an abundance of O atoms early in the time history. The NO-rich mixtures emphasize both reaction 12 and the NO catalytic effect in reaction 5. Estimates based on measurements⁽¹⁵⁾ below 2000° K indicated that the bimolecular path (reaction 11-12) should be unimportant above 3000° K, but this proved inconsistent with the present experimental results. In achieving a satisfactory fit, we have made use of recent high temperature measurements⁽¹⁶⁾ of the bimolecular rate constant.

A summary of the rate constants for reactions 1-12 is given in Table I.

Acknowledgements

The authors wish to acknowledge the support given to this work by Dr. M. Camac during the early stages of the experiment. They also wish to thank Mr. A. Magro for his devoted help in the actual operation of the shock tube.

REFERENCES

1. K. Wray, J.D. Teare, B. Kivel and P. Hammerling, Avco-Everett Research Laboratory, Research Report 83, December 1959.
2. P. Hammerling, J.D. Teare, B. Kivel, Phys. Fluids 2, 422 (1959).
3. M. Camac and A. Vaughan, J. Chem. Phys. 34, (1961).
4. V.H. Blackman, J. Fluid Mech. 1, 61 (1956).
5. M. Camac, J. Chem. Phys. 34, (1961).
6. F. Robben, J. Chem. Phys. 31, 420 (1959).
7. H. A. Bethe and E. Teller, Ballistic Research Laboratory, Report X-117 (1941).
8. E. Montroll and K. Shuler, J. Chem. Phys. 26, 454 (1957).
9. L. Landau and E. Teller, Physik. Z. Sowjetunion 10, 34 (1936).
10. R.N. Schwartz, Z. I. Slawsky and K. F. Herzfeld, J. Chem. Phys. 20, 1591 (1952). R. N. Schwartz and K. F. Herzfeld, J. Chem. Phys. 22, 767 (1954).
11. D. Britton, N. Davidson, and Schott, Discussions Faraday Soc. 17, 58 (1954).
12. E. Watanabe, M. Zelikoff, and E. C. Y. Inn, Geophysical Research Papers, No. 21, AFCRC Technical Report No. 53-23.
13. O.K. Rice, J. Chem. Phys. 4, 367 (1936).
14. Dulmage, Meyers, and Lipscomb, J. Chem. Phys. 19, 1432 (1951).
15. F. Kaufman, and J. Kelso, J. Chem. Phys. 23, 1702 (1955).
16. E. Freedman and J. Daiber, Unpublished, Cornell Aeronautical Laboratory, Buffalo, New York.

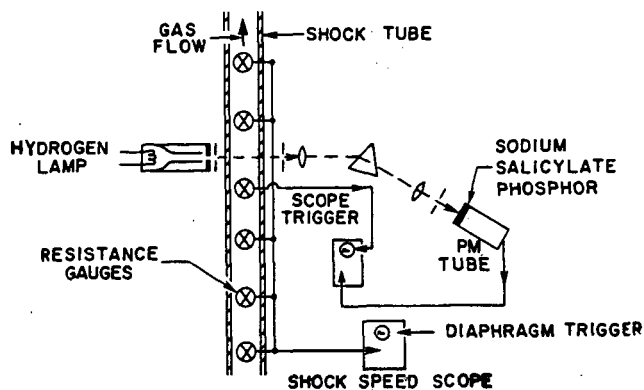


Fig. 1 Schematic diagram of the apparatus used in the ultraviolet light absorption experiments.

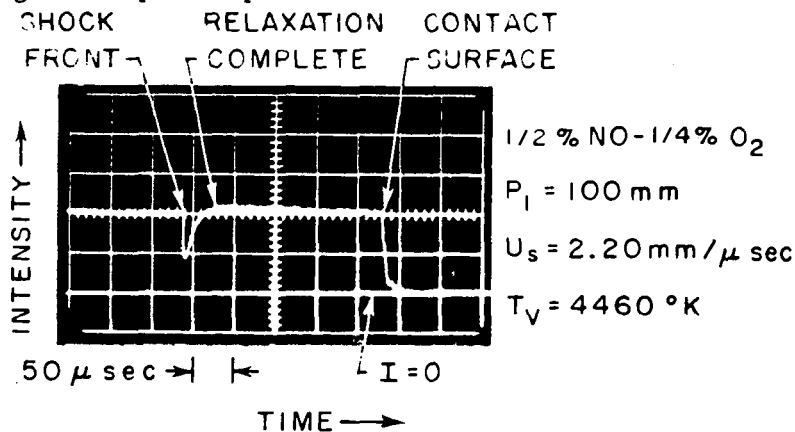


Fig. 2 Typical oscillogram from U. V. absorption experiments showing complete testing time.

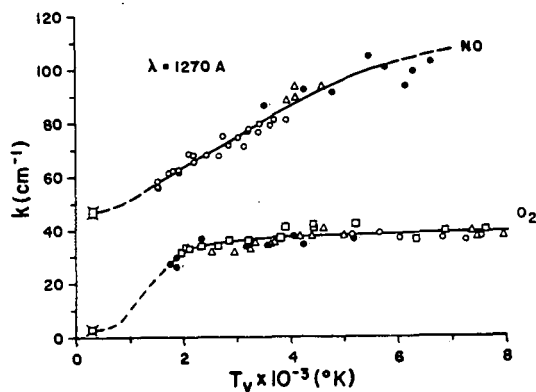


Fig. 3 Absorption coefficients of NO and O_2 per cm. of path length at a density corresponding to $P = 1 \text{ atm}$ and $T = 300^\circ \text{ K}$.

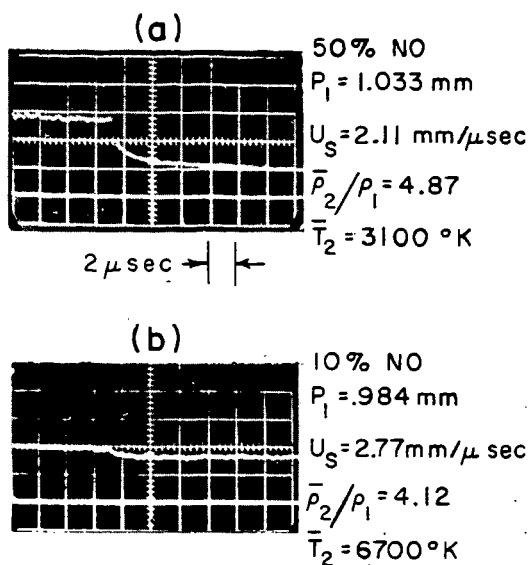


Fig. 4 Typical oscillograms showing the vibrational relaxation of NO.

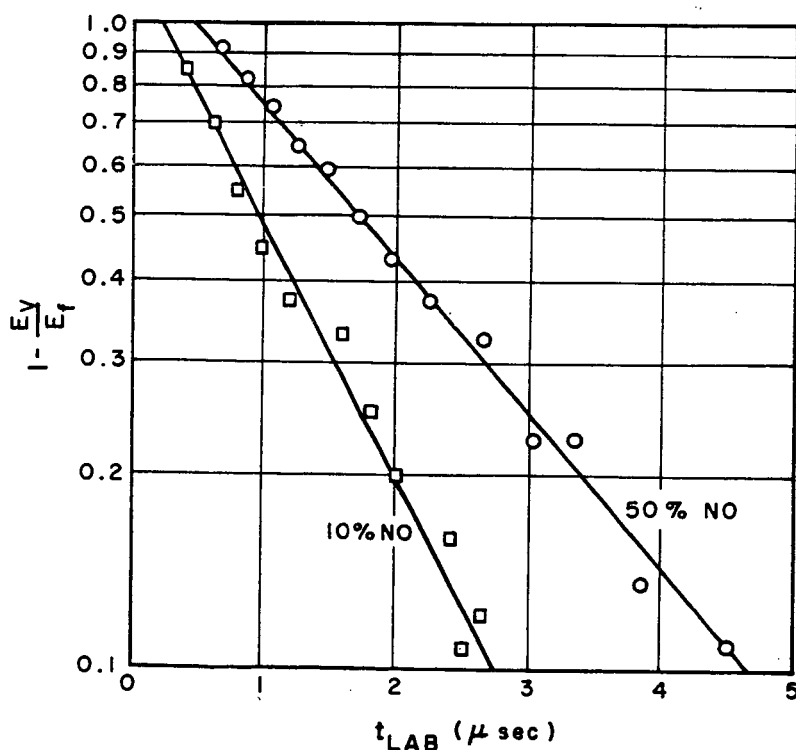


Fig. 5 Experimental plot of $1 - E_v/E_f$ against laboratory time. The two cases shown result from the oscillograms of Fig. 4.

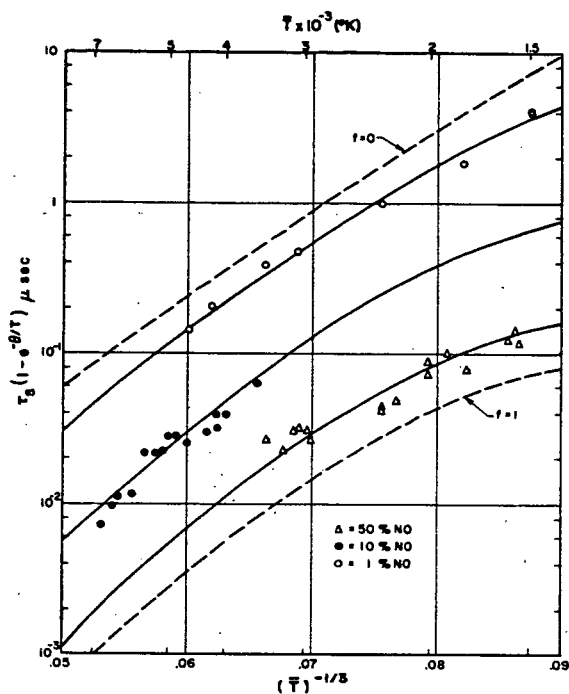


Fig. 6 Experimental vibrational (particle) times standardized to normal density. The solid curves are fitted to the data according to the theory of Schwartz, Slawsky and Herzfeld. The dashed curves show the deduced values of τ for NO-NO ($f=1$) and NO-Ar ($f=0$) collisions.

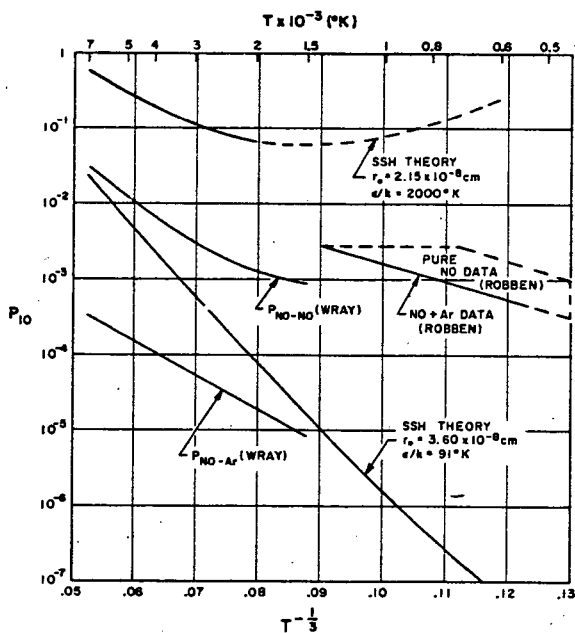


Fig. 7 Experimental and theoretical transition probabilities for de-exciting the first vibrational level of NO.

TABLE I - RATE CONSTANTS FOR CHEMICAL PROCESSES

Reaction	Catalyst M	Rate Constant
$O_2 + M + 5.1 \text{ ev} \xrightleftharpoons[k_R]{k_D} O + O + M$	Ar, N, N ₂ , NO	$k_D = \frac{3.6 \times 10^{18}}{T} \exp(-59373/T) \text{ cm}^3/\text{mole sec}$
	O ₂	$k_D = \frac{3.2 \times 10^{19}}{T} \exp(-59373/T) \text{ cm}^3/\text{mole sec}$
	O	$k_D = \frac{8.9 \times 10^{19}}{T} \exp(-59373/T) \text{ cm}^3/\text{mole sec}$
$N_2 + M + 9.8 \text{ ev} \xrightleftharpoons[k_R]{k_D} N + N + M$	Ar, O, O ₂ , NO	$k_R = 1.7 \times 10^{14} \times (T/4500)^{-1.5} \text{ cm}^6/\text{mole}^2 \text{ sec}$
	N ₂	$k_R = 5 \times 10^{14} \times (T/4500)^{-1.5} \text{ cm}^6/\text{mole}^2 \text{ sec}$
	N	$k_R = 8 \times 10^{15} \times (T/4500)^{-1.5} \text{ cm}^6/\text{mole}^2 \text{ sec}$
$NO + M + 6.5 \text{ ev} \xrightleftharpoons[k_R]{k_D} N + O + M$	Ar, O ₂ , N ₂	$k_R = 3.3 \times 10^{14} \times (T/4500)^{-1.5} \text{ cm}^6/\text{mole}^2 \text{ sec}$
	NO, O, N	$k_R = 6.7 \times 10^{15} \times (T/4500)^{-1.5} \text{ cm}^6/\text{mole}^2 \text{ sec}$
$NO + O + 1.4 \text{ ev} \xrightleftharpoons[k_2]{k_1} O_2 + N$	$k_2 = 1 \times 10^{12} T^{0.5} \exp(-3120/T)$	$\text{cm}^3/\text{mole sec}$
$N_2 + O + 3.3 \text{ ev} \xrightleftharpoons[k_2]{k_1} NO + N$	$k_2 = 1.3 \times 10^{13}$	$\text{cm}^3/\text{mole sec}$
$N_2 + O_2 + 1.9 \text{ ev} \xrightleftharpoons[k_2]{k_1} NO + NO$	$k_2 = 2.6 \times 10^{23} \times T^{-2.5} \exp(-43030/T)$	$\text{cm}^3/\text{mole sec}$